

Strong Magnetic Fields and Pasta Phases Reexamined

Luigi Scurto, Helena Pais, Francesca Gulminelli

26ème Congrès Général de la Société Française de Physique



Table of Contents

- ◆ Introduction
- ◆ Theoretical Framework
- ◆ Results
- ◆ Conclusions

Introduction

Neutron Stars

Neutron Stars are astrophysical objects of extreme interest in the new multimessenger era of astronomy



Credits: ESO/L. Calçada

Neutron Stars

Neutron Stars are astrophysical objects of extreme interest in the new multimessenger era of astronomy



Credits: ESO/L. Calçada

◆ Magnetic Fields up to $\approx 10^{15}G$ on the surface,

Neutron Stars

Neutron Stars are astrophysical objects of extreme interest in the new multimessenger era of astronomy

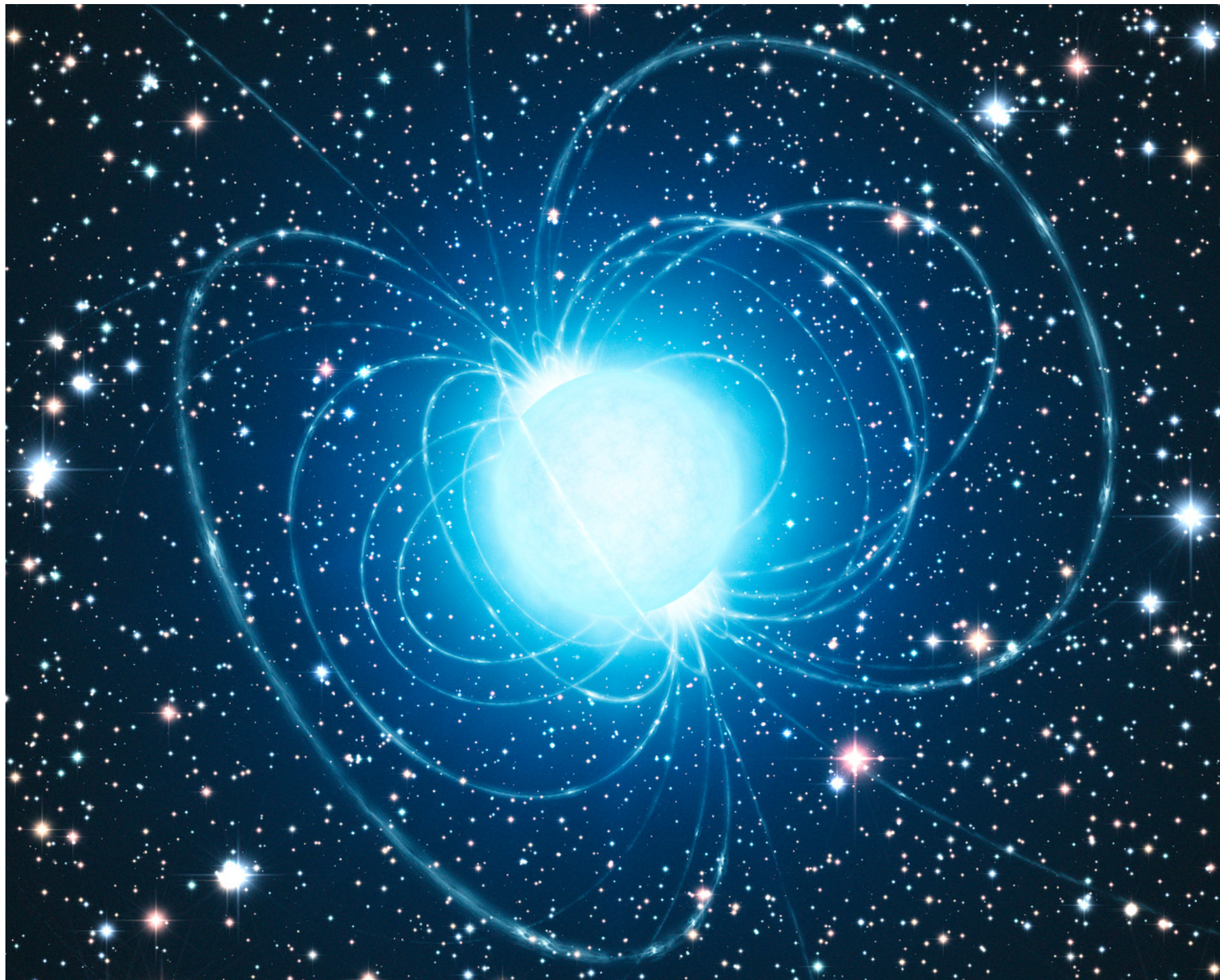


Credits: ESO/L. Calçada

- ◆ Magnetic Fields up to $\approx 10^{15} G$ on the surface,
- ◆ Central densities up to several times ρ_0 ,

Neutron Stars

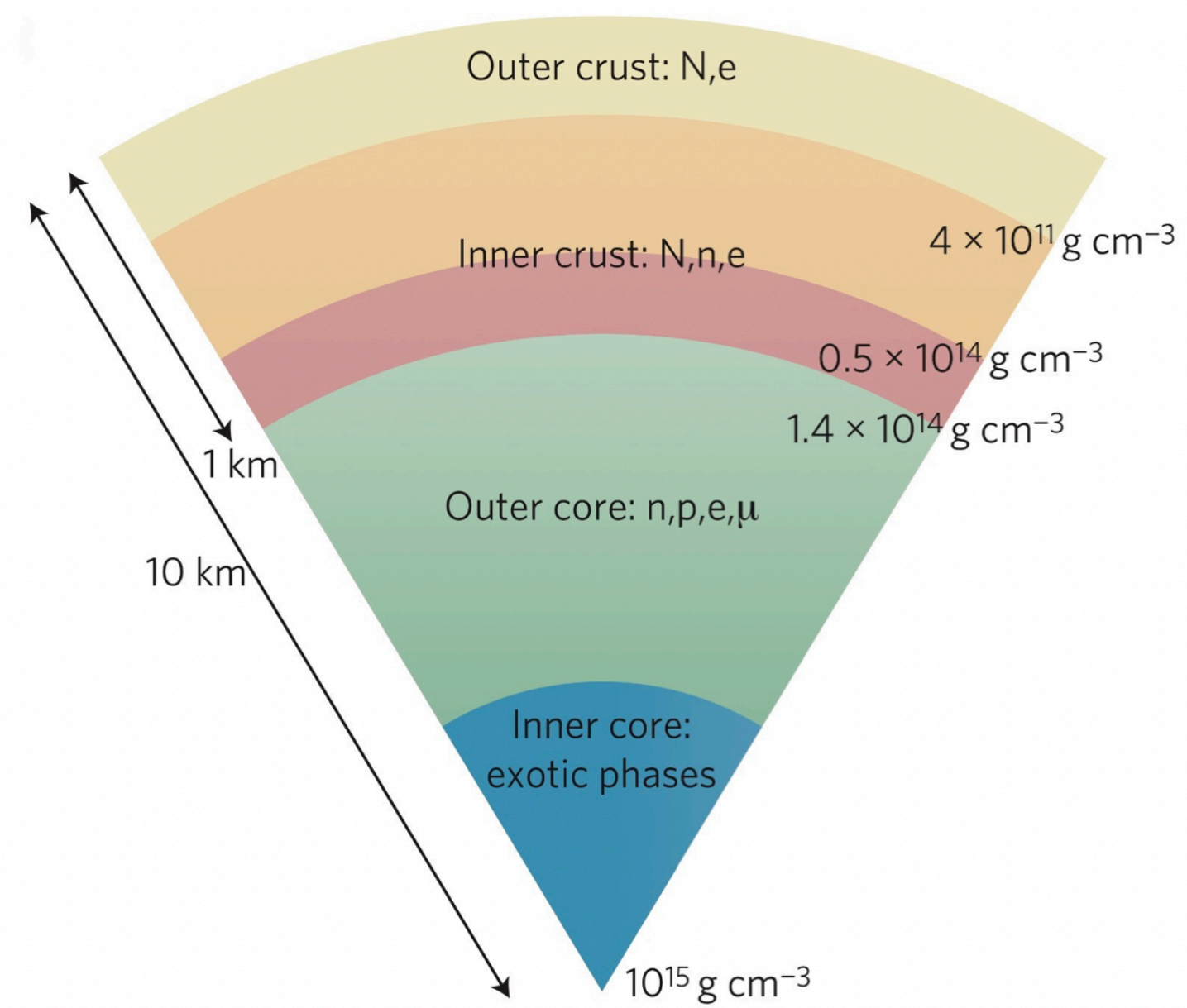
Neutron Stars are astrophysical objects of extreme interest in the new multimessenger era of astronomy



- ◆ Magnetic Fields up to $\approx 10^{15} G$ on the surface,
- ◆ Central densities up to several times ρ_0 ,
- ◆ Strongly asymmetric matter ($\rho_p \ll \rho_n$)

Credits: ESO/L. Calçada

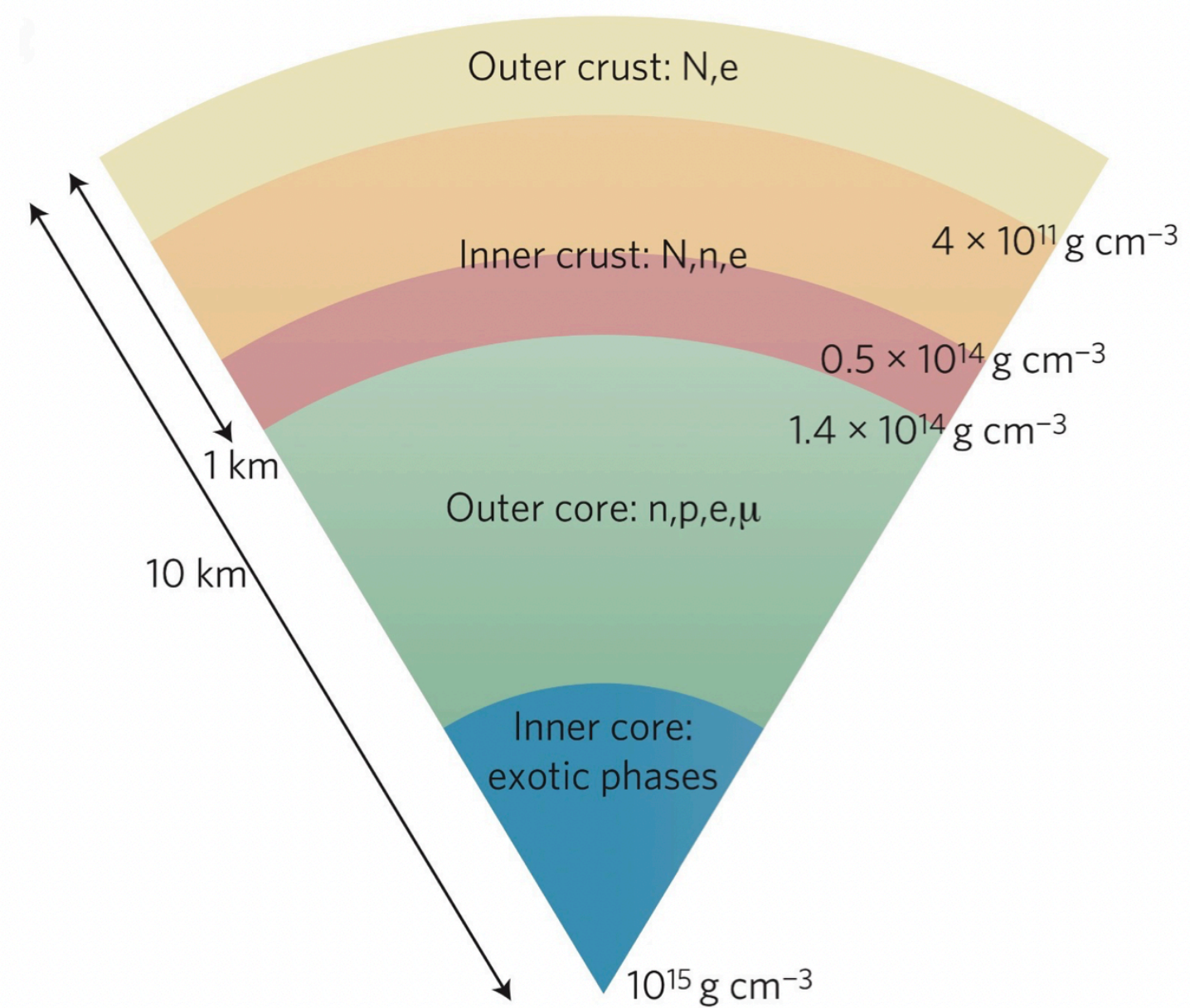
The Interior of a Neutron Star



The interior of a NS is considered to be divided into 3 main layers

Credits: Credits: G.W.Newton, Nature Physics, 9:396–397, July 2013.

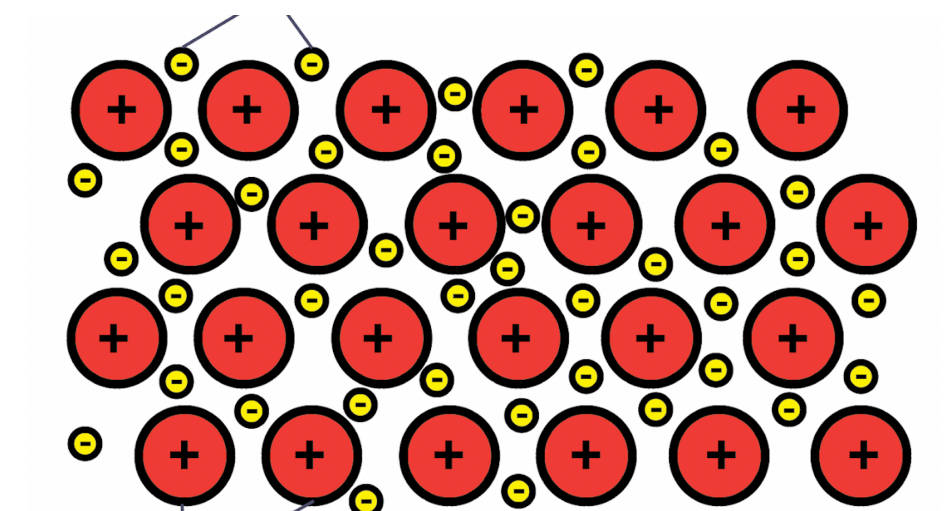
The Interior of a Neutron Star



The interior of a NS is considered to be divided into 3 main layers

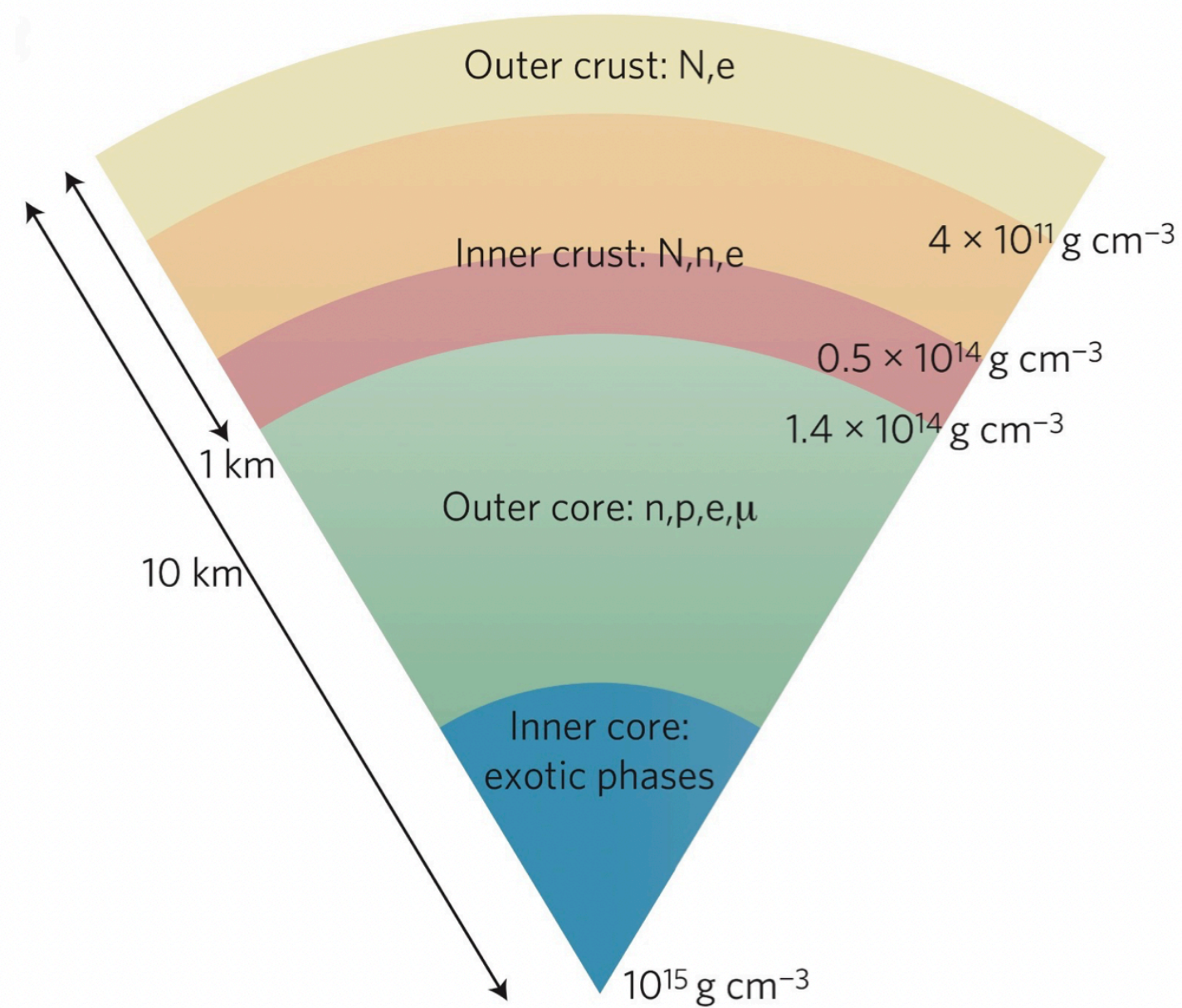
◆ Outer Crust

Credits: Credits: G.W.Newton, Nature Physics, 9:396–397, July 2013.



Credits: Credits: IGCSE Chemistry 2017

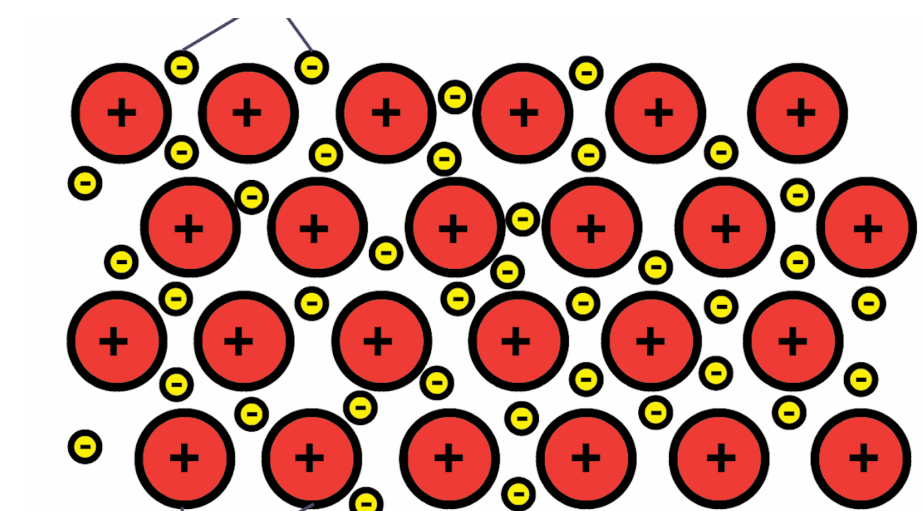
The Interior of a Neutron Star



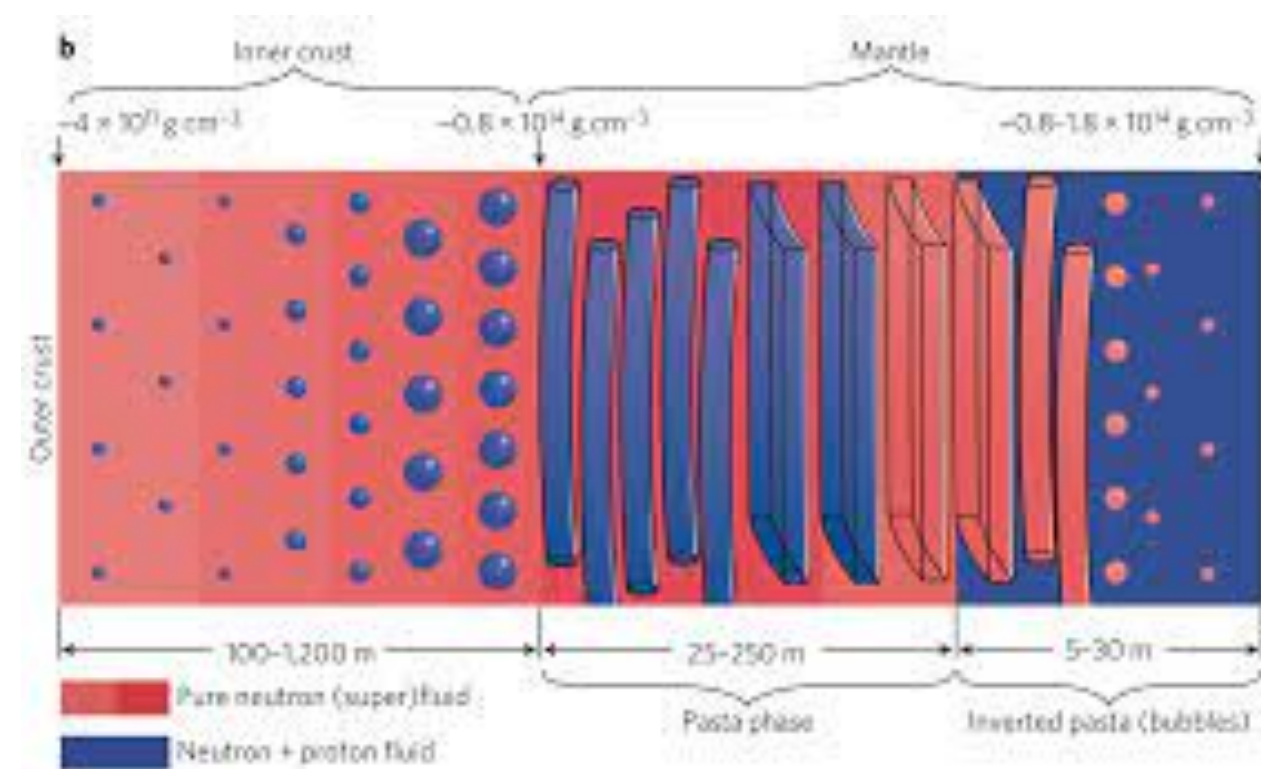
The interior of a NS is considered to be divided into 3 main layers

- ◆ Outer Crust
- ◆ Inner Crust

Credits: Credits: G.W. Newton, Nature Physics, 9:396–397, July 2013.

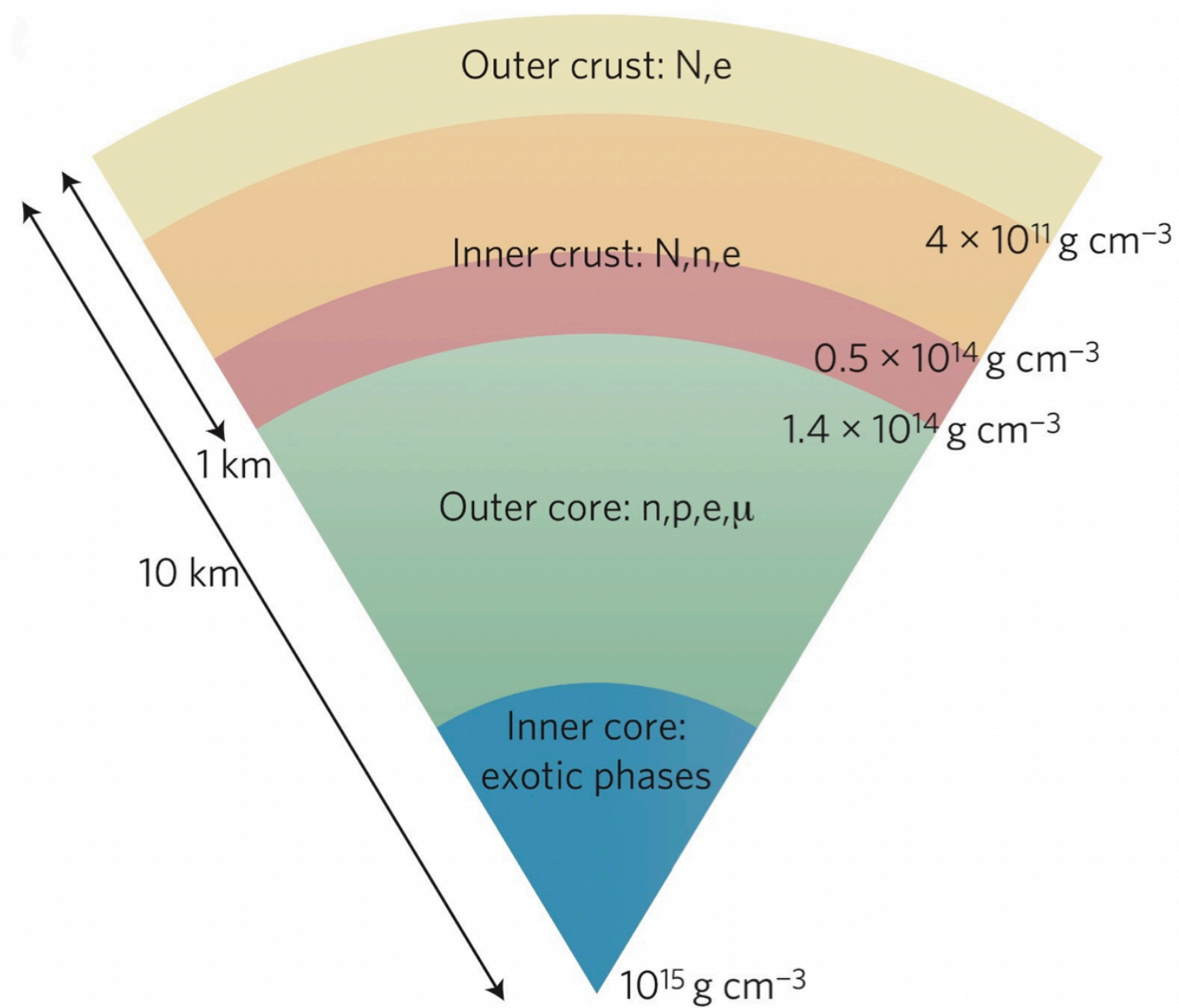


Credits: Credits: IGCSE Chemistry 2017



Credits: G.W. Newton, Nature Physics, 9:396–397, July 2013.

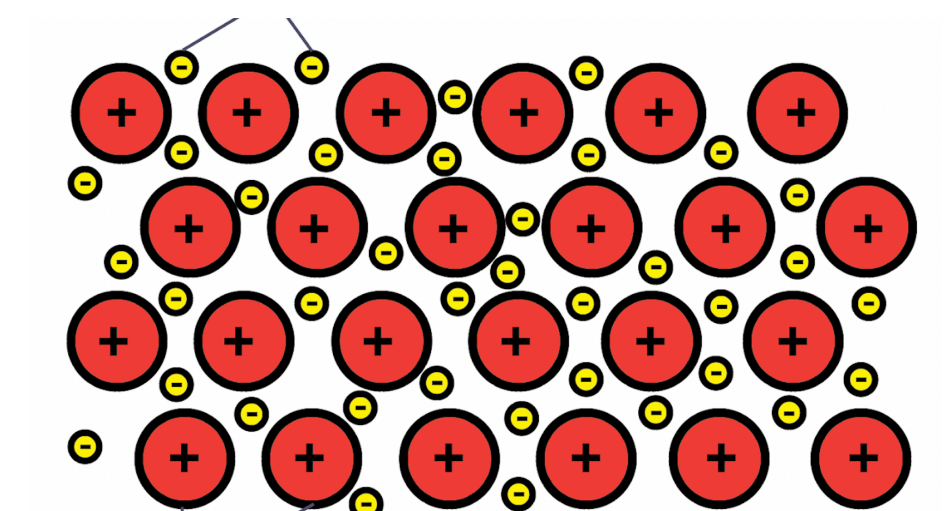
The Interior of a Neutron Star



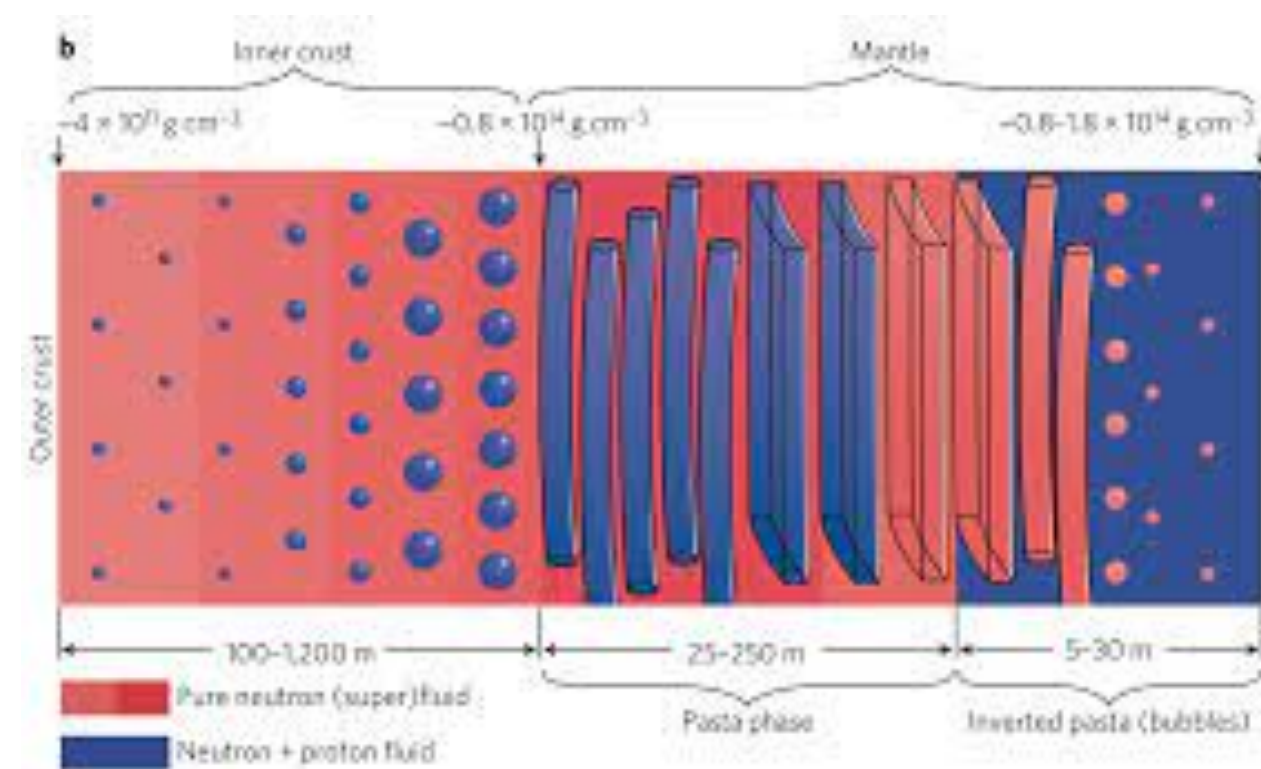
The interior of a NS is considered to be divided into 3 main layers

- ◆ Outer Crust
- ◆ Inner Crust
- ◆ Core

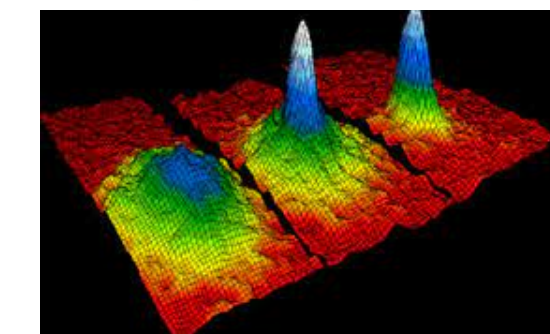
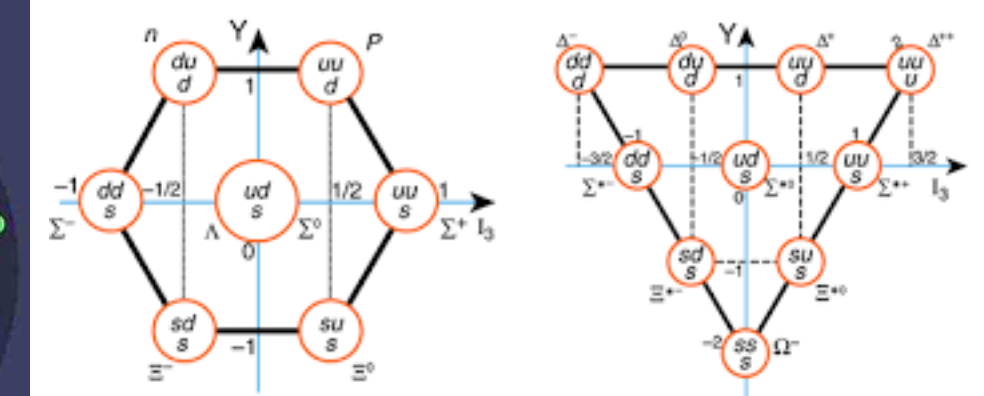
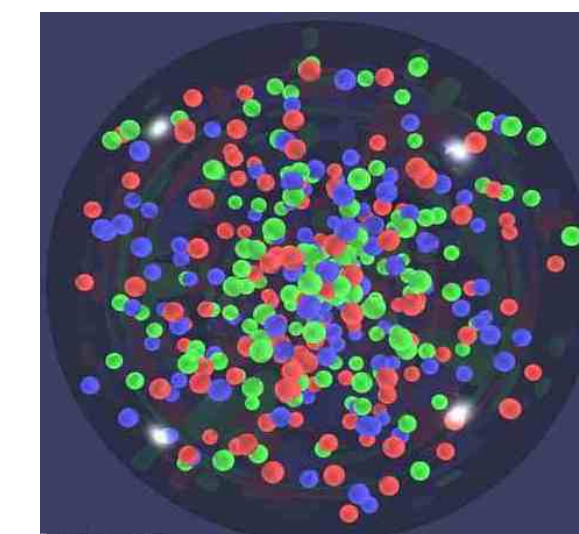
Credits: G.W.Newton, Nature Physics, 9:396–397, July 2013.



Credits: IGCSE Chemistry 2017



Credits: G.W.Newton, Nature Physics, 9:396–397, July 2013.



Credits: E.A.Cornell et al., H. Lenske & M. Dhar, F.Cain

Theoretical Framework

Relativistic Mean Field Models

In our work we use two different Relativistic Mean Field (RMF) models in order to describe stellar matter (npe). In this approximation, the interaction between nucleons is mediated by mesons.

$$\mathcal{L} = \underbrace{\sum_{i=p,n} \mathcal{L}_i}_{\text{Nucleons}} + \underbrace{\mathcal{L}_e}_{\text{Electrons}} + \underbrace{\mathcal{L}_\sigma + \mathcal{L}_\omega + \mathcal{L}_\rho + \mathcal{L}_{nl}}_{\text{Mesons + self-interactions}} + \underbrace{\mathcal{L}_A}_{\text{EM Field}}$$

In our study we use the NL3 and NL3 $\omega\rho$ models, which only differ for the value of the slope of the symmetry energy L , namely $L = 118\text{MeV}$ and $L = 55\text{MeV}$.

We always consider $A^\mu = (0,0,Bx,0)$ and we define $B^* = B/B_c$, with $B_c = 4.414 \cdot 10^{13}\text{G}$.

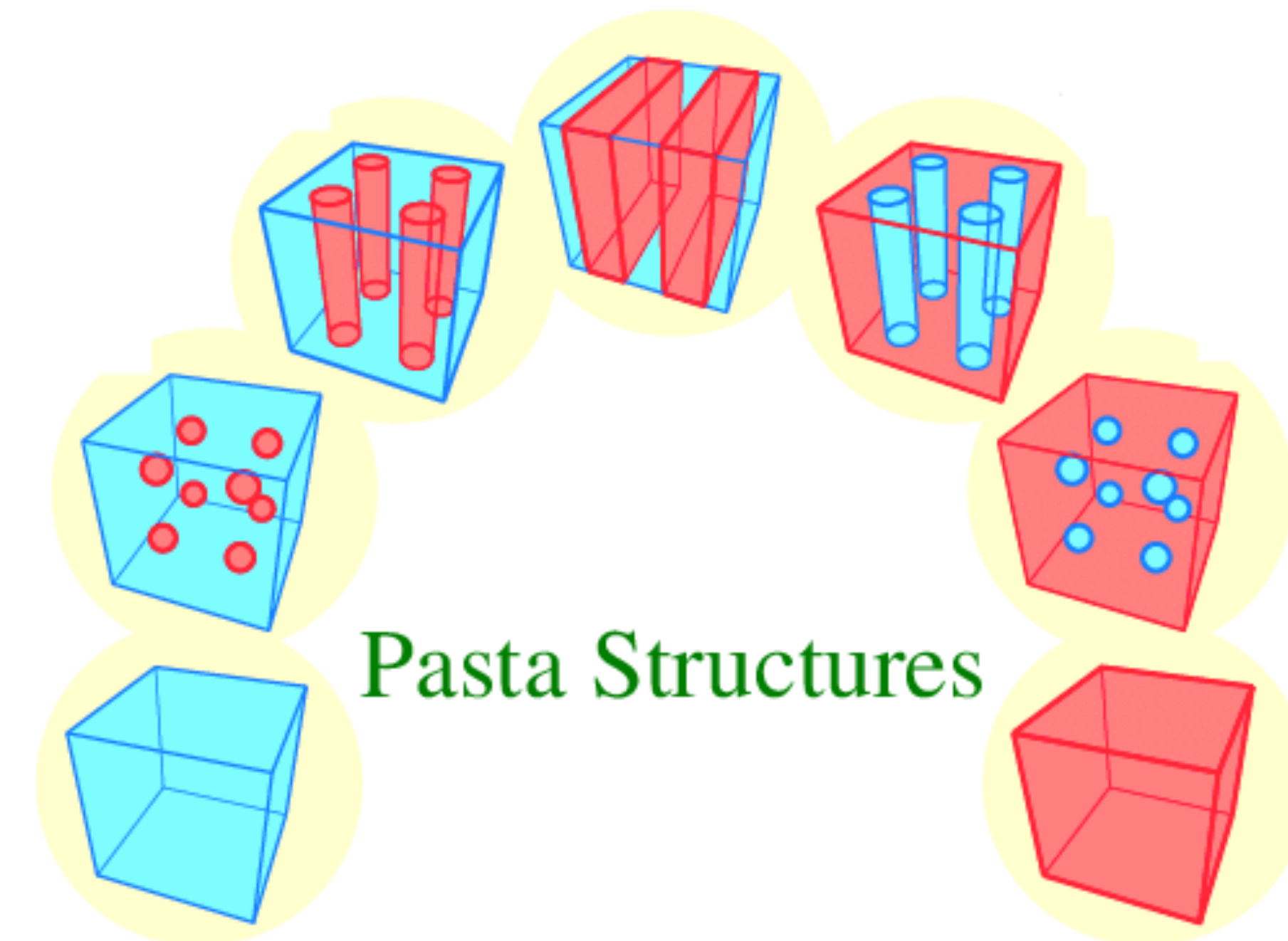
Pasta Phases

In order to describe the heavy clusters inside the IC of the star, we use two different models:

- **Coexisting Phases (CP) Model**
- **Compressible Liquid Drop (CLD) Model**

In both models we consider our system as a mixture of two phases, a denser (liquid) one and a less dense (gas) phase. Each one of the two phases has to fulfill its own set of meson Euler-Lagrange equations, and they have to fulfill some equilibrium conditions.

Also, in both models the each cluster is considered to be in the center of a Wiegner-Seitz(WS) cell.



Credits: Tatsumi, Toshitaka and Tomoki, Endo and Chiba, Satoshi, (2006)

Coexisting Phases (CP) Model

In this model the equilibrium between the two phases is imposed through the relations:

$$\mu_p^I = \mu_p^{II}$$

$$\mu_n^I = \mu_n^{II}$$

$$P^I = P^{II}$$

After the equilibrium conditions are imposed, we include corrections to the energy density so that its final equation is

$$\mathcal{E} = f\mathcal{E}^I + (1 - f)\mathcal{E}^{II} + \mathcal{E}_{Coul} + \mathcal{E}_{surf} + \mathcal{E}_e.$$

Where

f = fraction of liquid phase

\mathcal{E}^i = energy density of phase I

\mathcal{E}_e = energy density of electrons

$$\mathcal{E}_{Coul} = 2\alpha e^2 \pi \Phi R_d^2 \left(\rho_p^I - \rho_p^{II} \right)^2$$

$$\mathcal{E}_{surf} = \frac{\sigma \alpha D}{R_d}$$

Compressible Liquid Drop (CLD) Model

In this case the Coulomb and Surface corrections come into play already before the minimization, so that the equilibrium conditions become

$$\mu_n^I = \mu_n^{II}$$

$$\mu_p^I = \mu_p^{II} - \frac{\mathcal{E}_{surf}}{f(1-f)(\rho_p^I - \rho_p^{II})}$$

$$P^I = P^{II} + \mathcal{E}_{surf} \left[\frac{3}{2\alpha} \frac{\partial \alpha}{\partial f} + \frac{1}{2\Phi} \frac{\partial \Phi}{\partial f} - \frac{((1-f)\rho_p^I + f\rho_p^{II})}{(1-f)f(\rho_p^I - \rho_p^{II})} \right]$$

Results

CP vs CLD

Our first result shows the main difference between the CP calculation, used in previous studies, and the CLD calculation used in our work.

RED

The energy per baryon of homogeneous matter is higher



Clusters are favored
(stable solution)

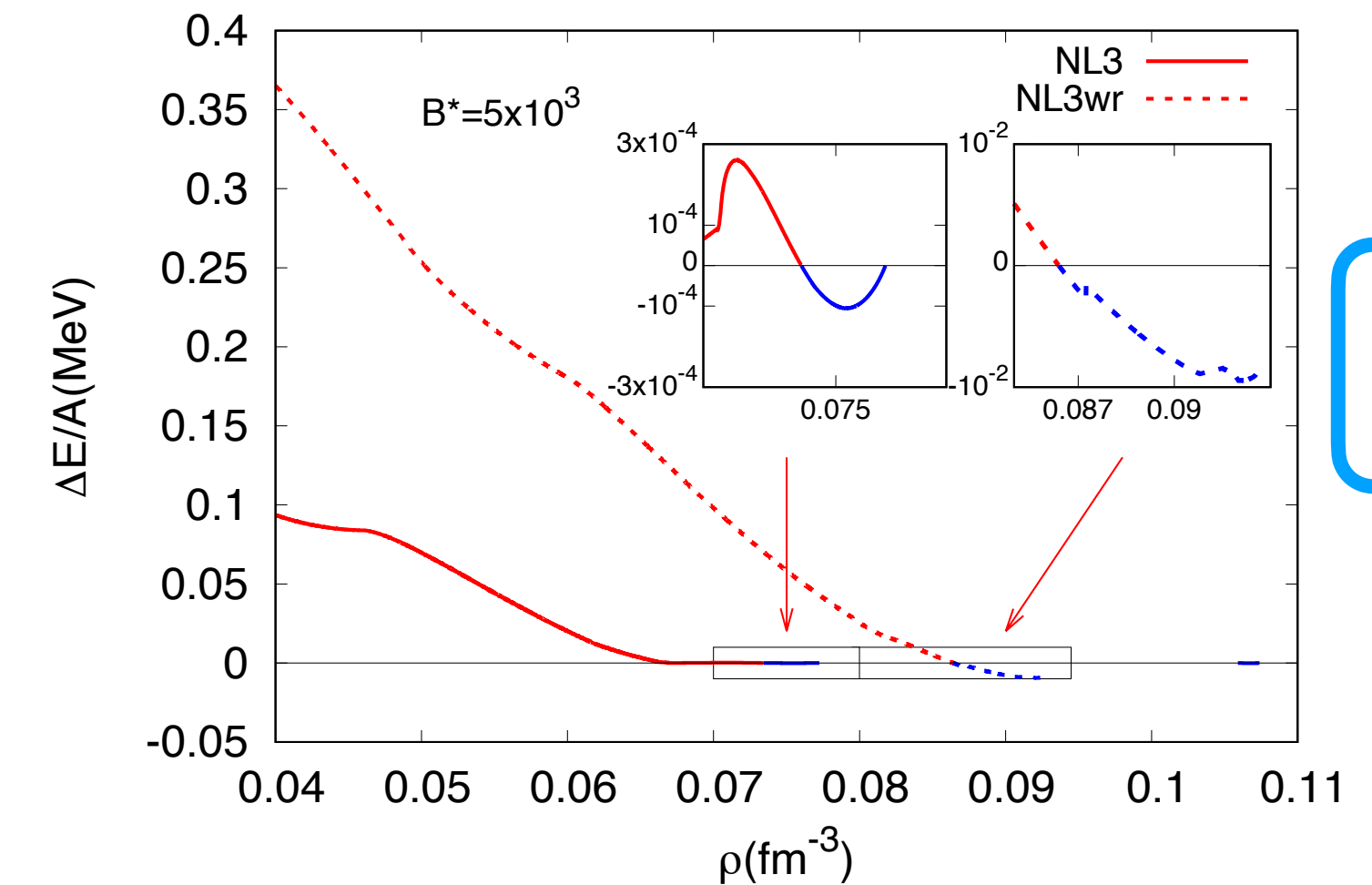
BLUE

The energy per baryon of inhomogeneous matter is higher

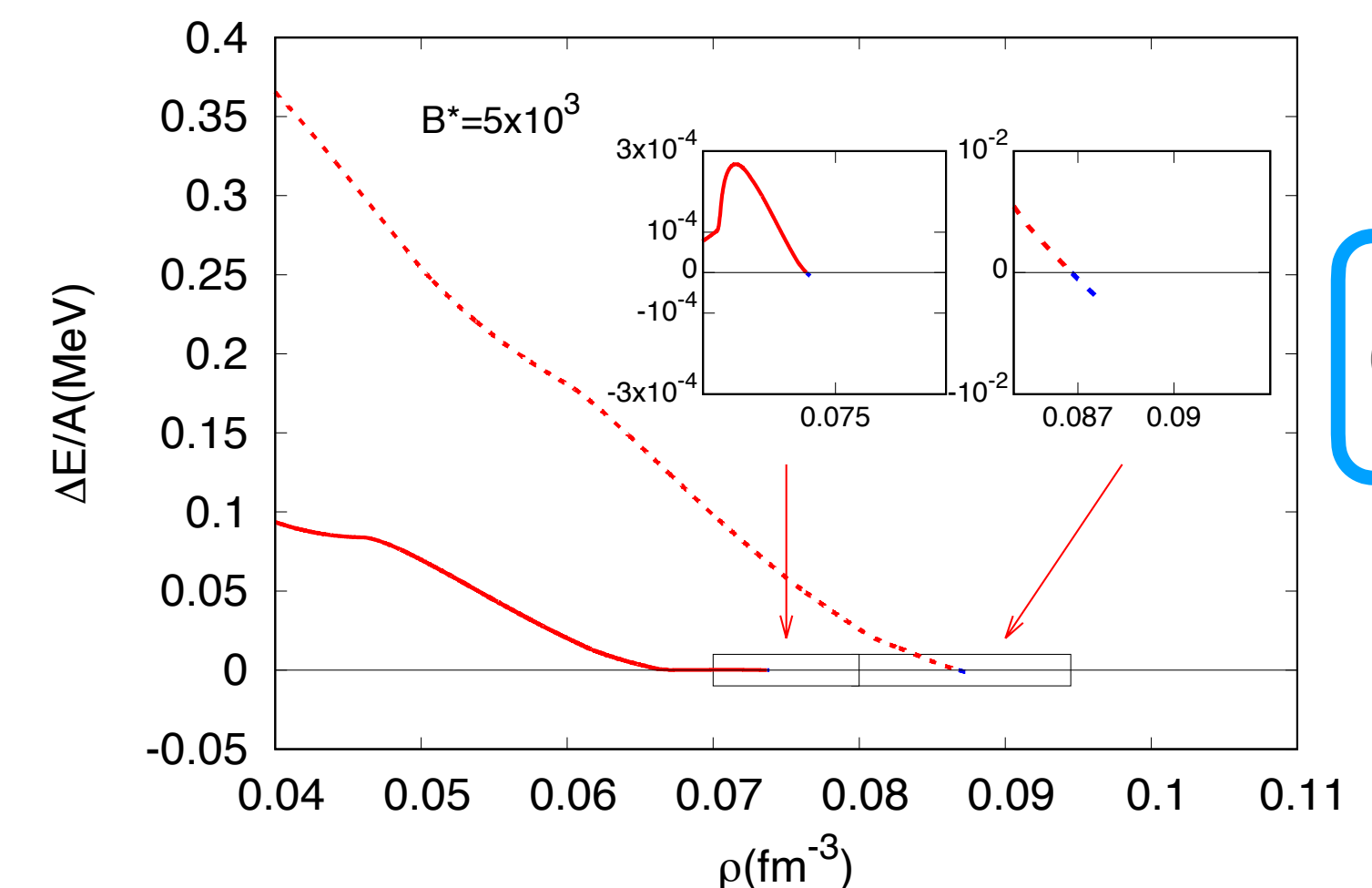


Homogeneous matter is favored.
(metastable solution)

In the CP model, metastable solutions are present, while they are almost completely absent in the CLD calculation



CP



CLD

Fig.1 Difference between the energy of homogeneous and inhomogeneous matter, in the CP (top) and CLD (bottom) calculations.

Extended Crust

In the case of the NL3 model, we observed that, due to the presence of the B field, the crust-core transition density (**orange** line in the plots) gets shifted to higher values with respect to the B=0 case (**green** line in the plots).

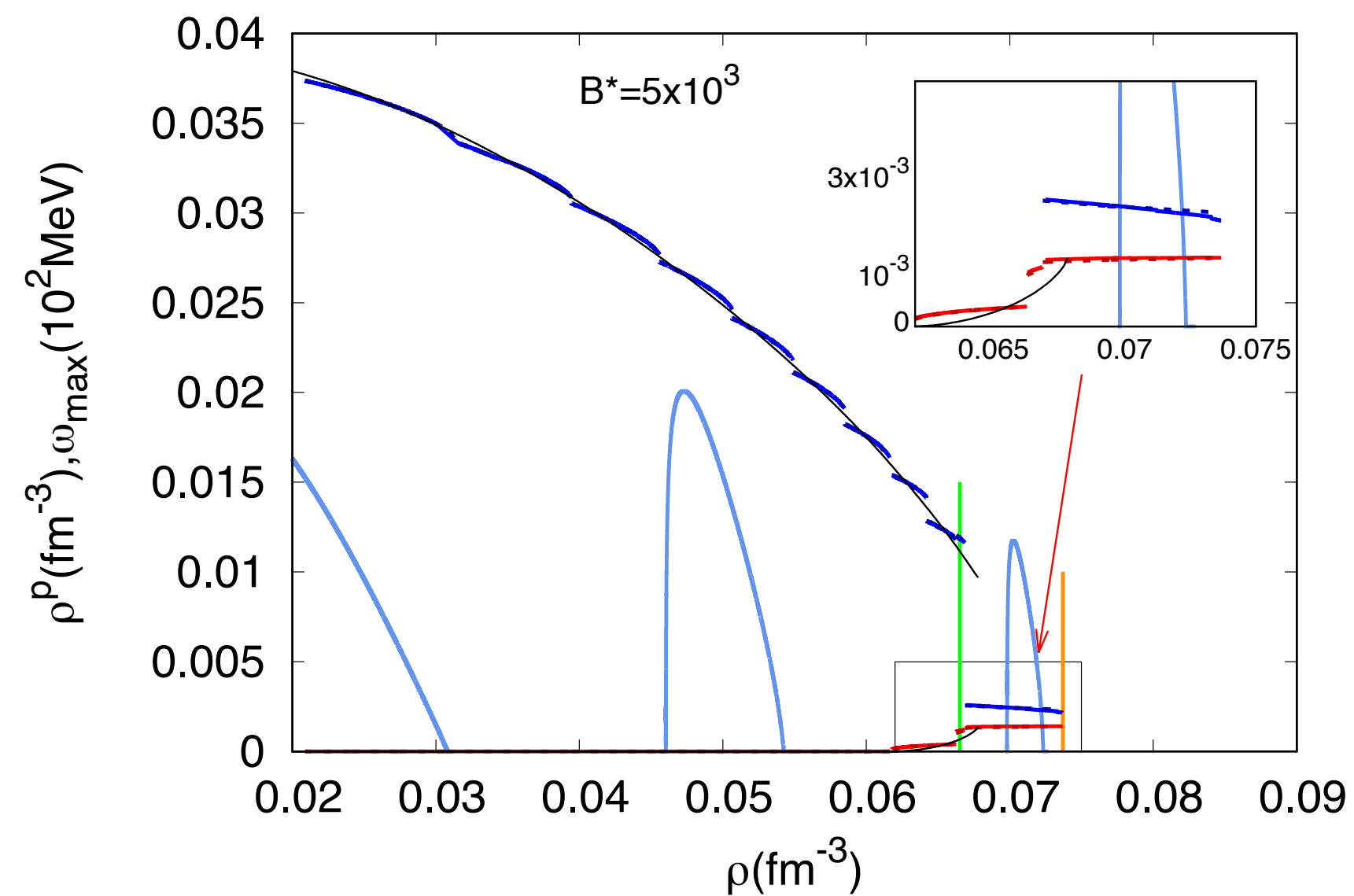


Fig.3 Proton density of liquid (blue) and gas (red) phase for the NL3 model.

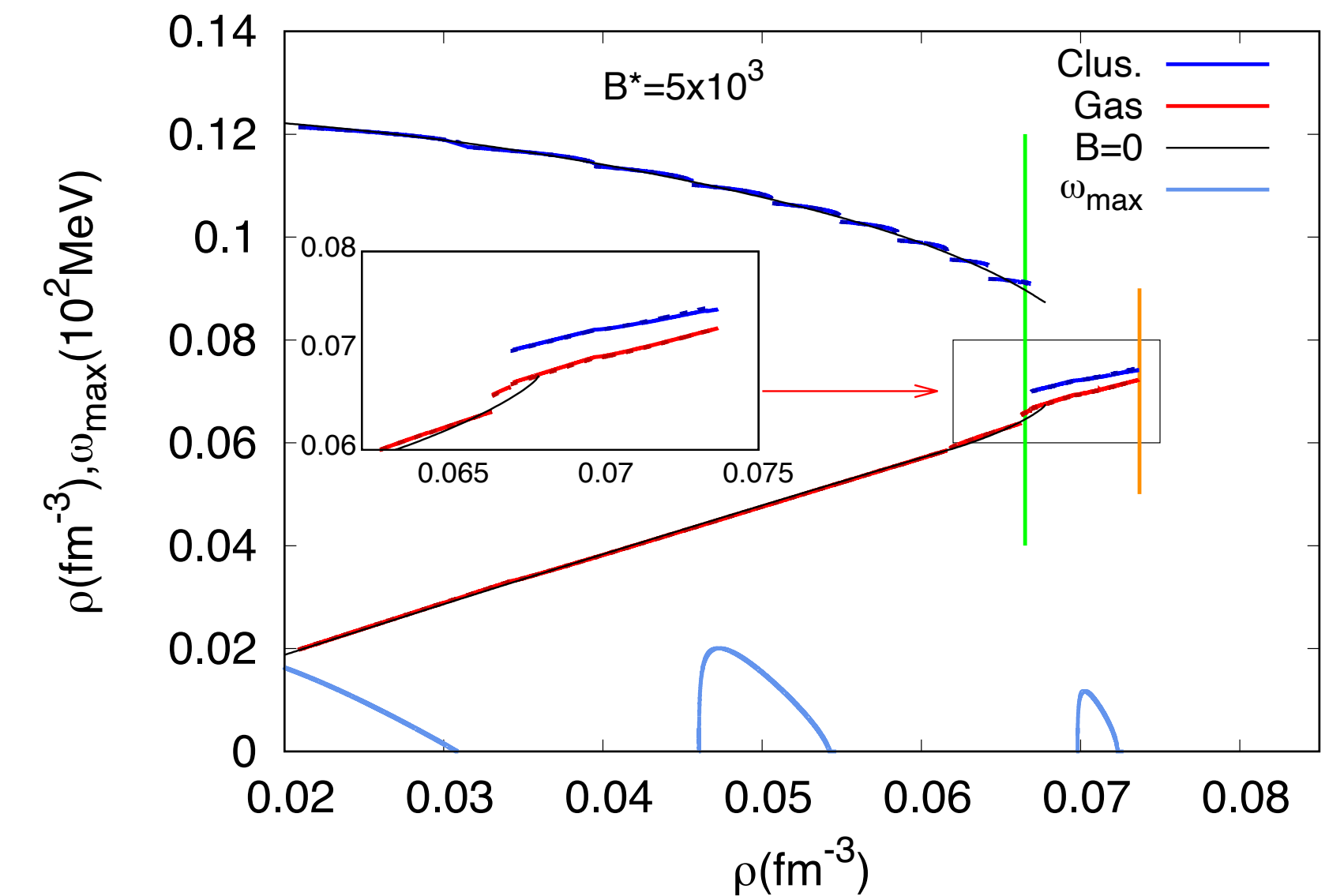


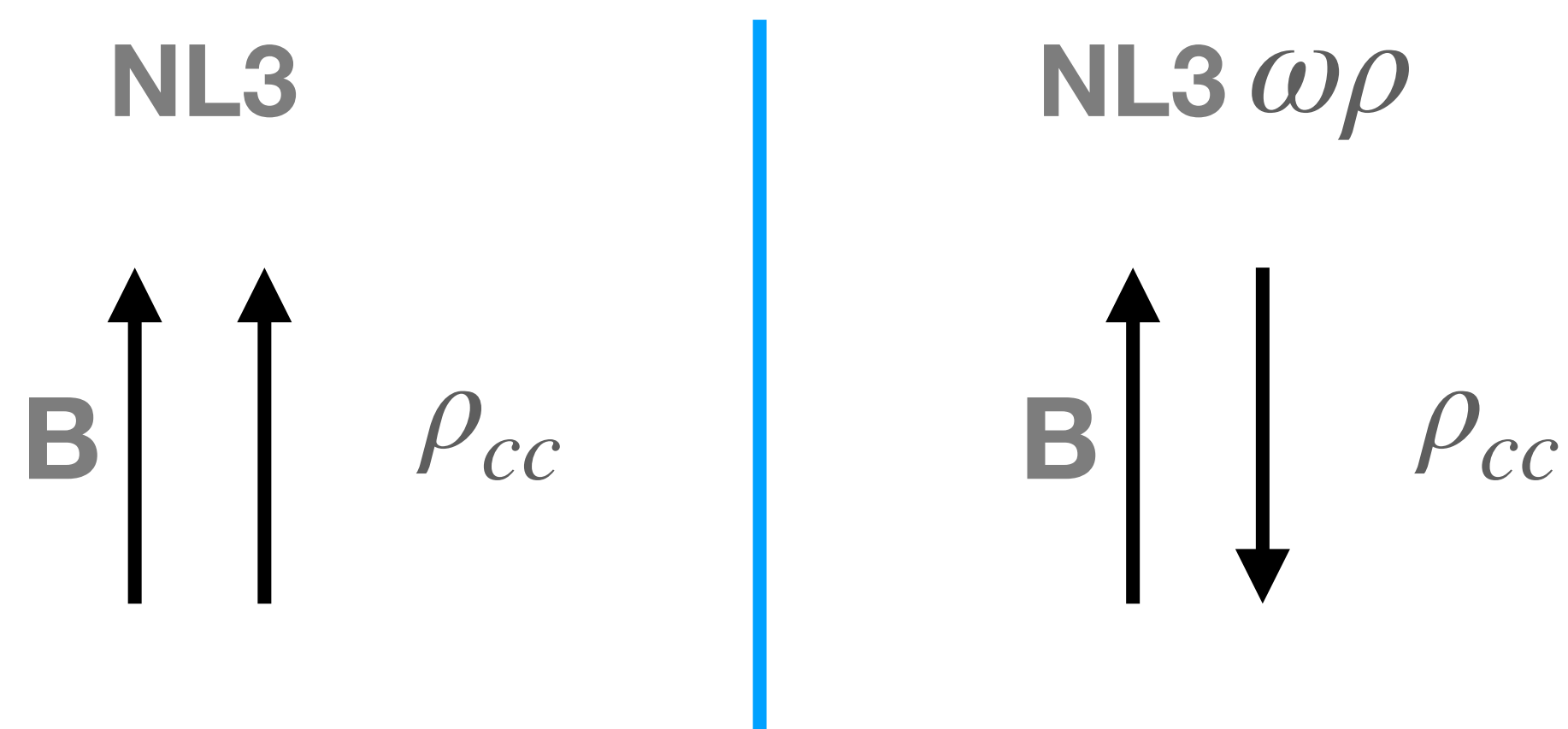
Fig.2 Baryon density of liquid (blue) and gas (red) phase for the NL3 model.

As already observed in previous studies, the new region of inhomogeneity is in good agreement with the results of a dynamical spinodal calculation (**light blue** lines in the plots).

Moreover, in the new region, the baryon and proton density of the liquid (**blue** in the plots) and gas (**red** in the plots) phases, become very similar.

Model Dependency

The previous result, however, appears to be model dependent, since in the NL3 $\omega\rho$ model, the role of the field appear to be the one of decreasing the crust-core transition density, and the new region of inhomogeneity does not appear



Where does this difference come from ?

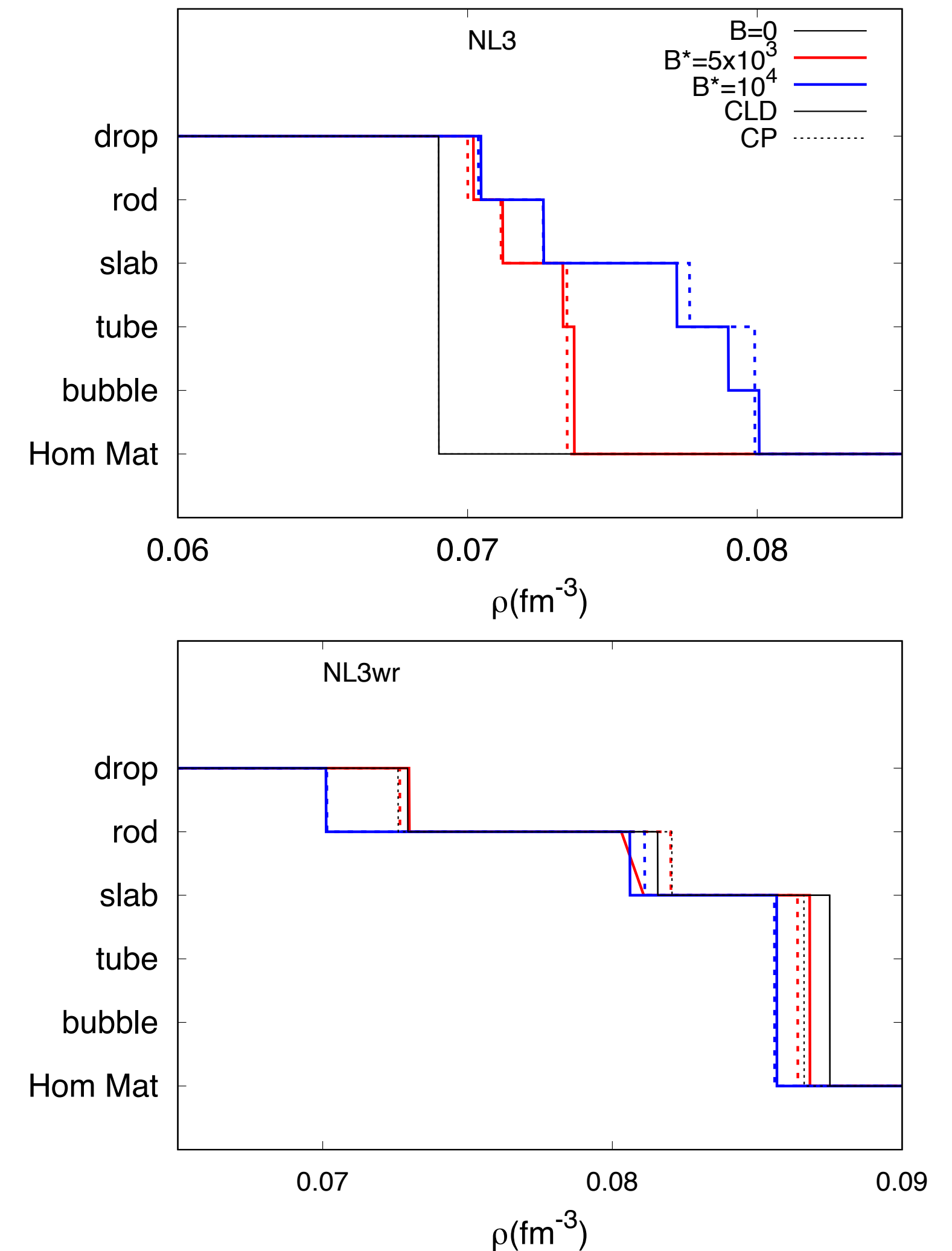
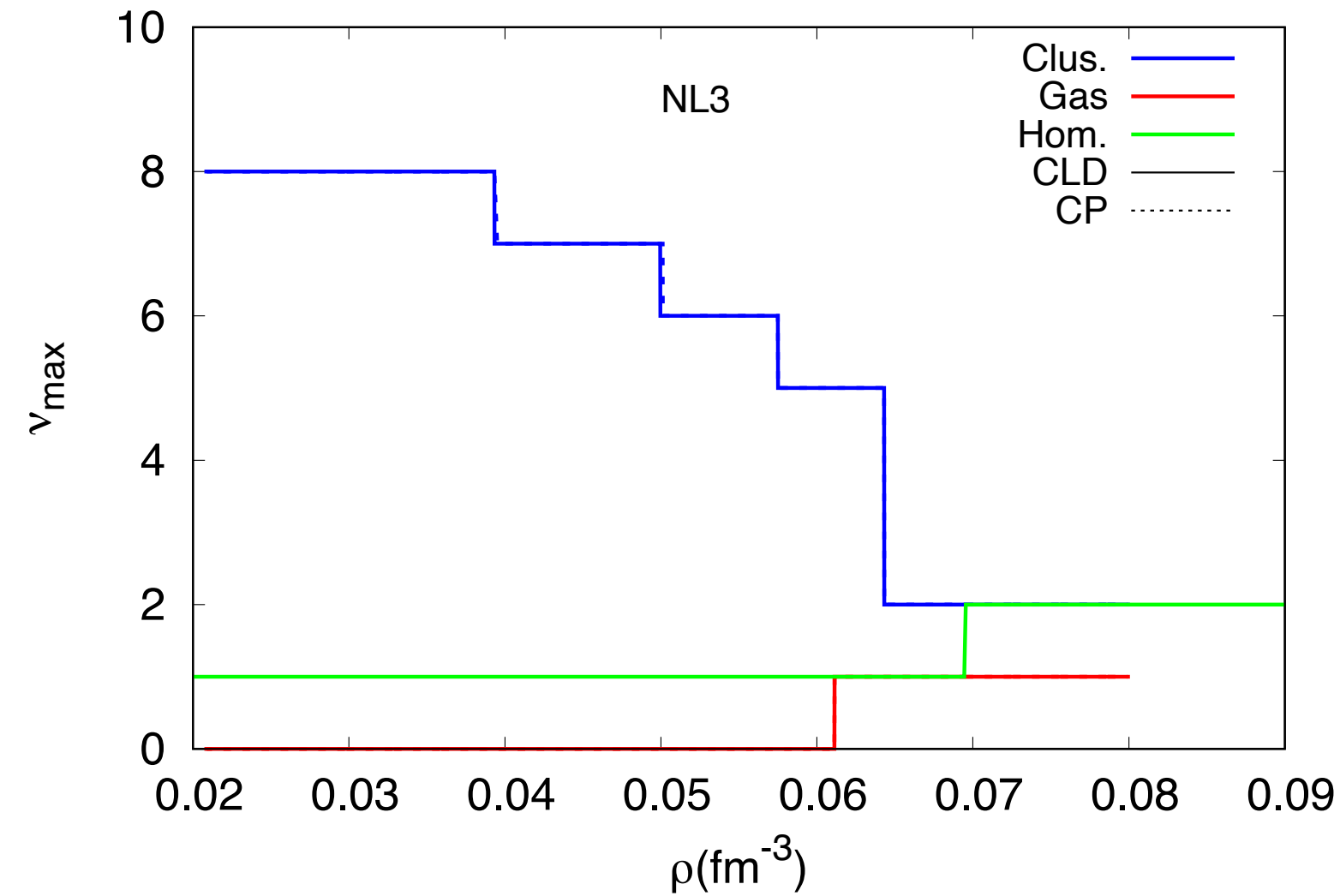


Fig.4 Cluster geometries for the NL3 (top) and NL3 $\omega\rho$ (bottom) models.

Model Dependency



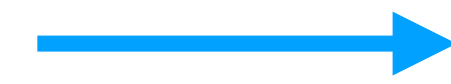
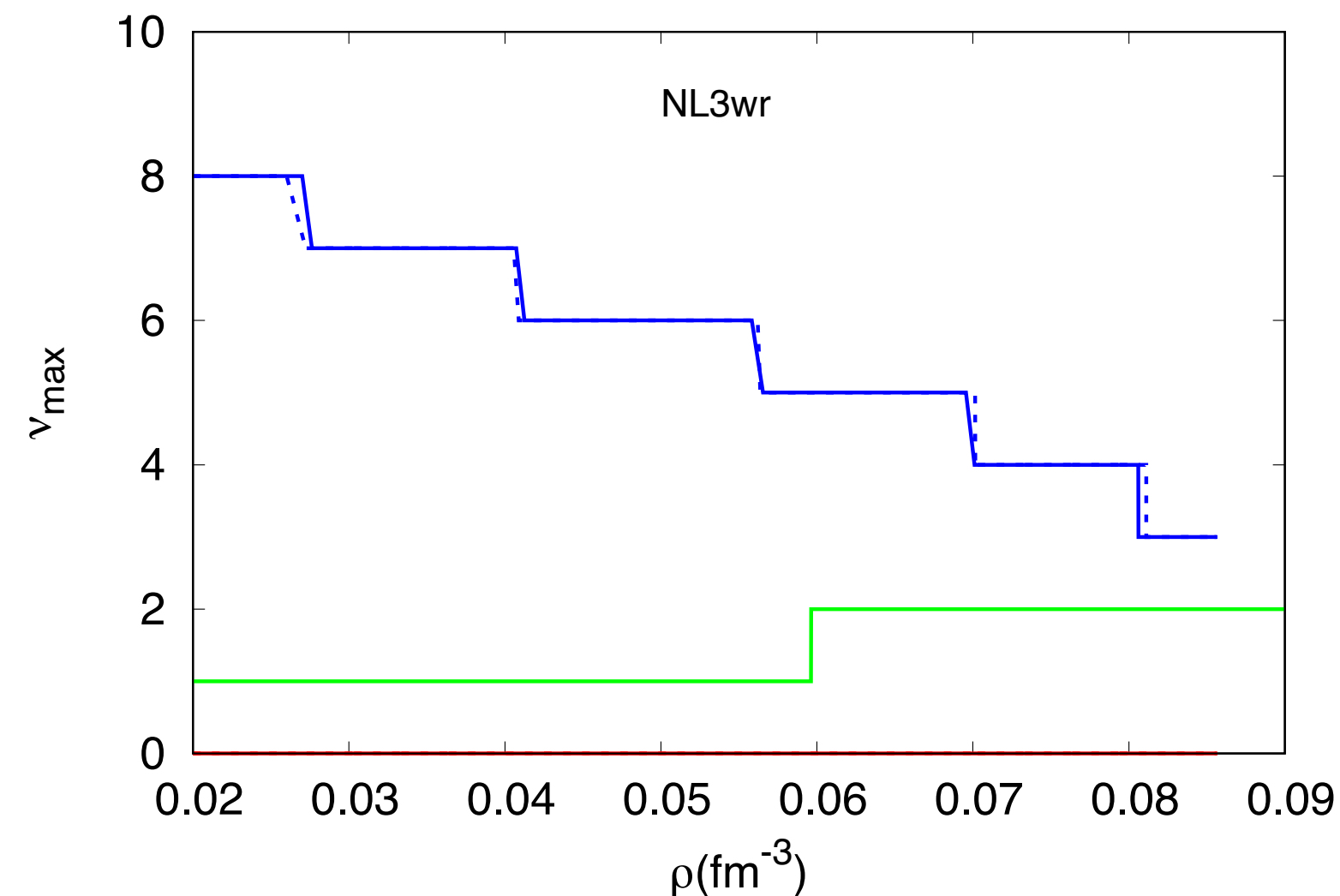
Different occupation of the Landau levels, due to the different proton fraction of the two models



Protons in the liquid phase (**blue**) occupy the same level as they would in homogeneous matter (**green**), but the one in the gas phase (**red**) occupy a lower level.



Inhomogeneity is favored



Protons in the liquid phase (**blue**) occupy an higher level with respect to the one they would occupy in homogeneous matter (**green**).



Homogeneous matter is favored

Fig.5 Highest occupied Landau level for the NL3 (top) and NL3 ω (bottom) models.

Conclusions

Conclusions

In our work we studied how a strong magnetic field affects the structure of the inner crust of a neutron star. In the study we used two different RMF models and the CLD calculation for the clusters.

From our work we can extract the following conclusions:

Conclusions

In our work we studied how a strong magnetic field affects the structure of the inner crust of a neutron star. In the study we used two different RMF models and the CLD calculation for the clusters.

From our work we can extract the following conclusions:

- ◆ The CLD calculation tends to eliminate metastable solutions that are present in the CP calculation,

Conclusions

In our work we studied how a strong magnetic field affects the structure of the inner crust of a neutron star. In the study we used two different RMF models and the CLD calculation for the clusters.

From our work we can extract the following conclusions:

- ◆ The CLD calculation tends to eliminate metastable solutions that are present in the CP calculation,
- ◆ In the NL3 model, an extended inhomogeneous region appears, in which the densities of the two phases become much closer to each other,

Conclusions

In our work we studied how a strong magnetic field affects the structure of the inner crust of a neutron star. In the study we used two different RMF models and the CLD calculation for the clusters.

From our work we can extract the following conclusions:

- ◆ The CLD calculation tends to eliminate metastable solutions that are present in the CP calculation,
- ◆ In the NL3 model, an extended inhomogeneous region appears, in which the densities of the two phases become much closer to each other,
- ◆ This extended region does not appear in the model with low slope of the symmetry energy. This should be caused by the different occupation of the Landau levels in the two models.

Strong magnetic fields and pasta phases reexamined

Luigi Scurto ^{1,*} Helena Pais ^{2,†} and Francesca Gulminelli ^{3,‡}

¹*CFisUC, Department of Physics, University of Coimbra, 3004-516 Coimbra, Portugal*

²*Department of Fundamental Physics, University of Salamanca, E-37008 Salamanca, Spain*

³*Normandie Université, ENSICAEN, UNICAEN, CNRS/IN2P3, LPC Caen, F-14000 Caen, France*

In this work, we compute the structure and composition of the inner crust of a neutron star in the presence of a strong magnetic field, such as can be found in magnetars. To determine the geometry and characteristics of the crust inhomogeneities, we consider the compressible liquid drop model, where surface and Coulomb terms are included in the variational equations, and we compare our results with previous calculations based on more approximate treatments. For the equation of state (EoS), we consider two nonlinear relativistic mean-field models with different slopes of the symmetry energy, and we show that the extension of the inhomogeneous region inside the star core due to the magnetic field strongly depends on the behavior of the symmetry energy in the crustal EoS. Finally, we argue that the extended spinodal instability observed in previous calculations can be related to the presence of small amplitude density fluctuations in the magnetar outer core, rather than to a thicker solid crust. The compressible liquid drop model formalism, while in overall agreement with the previous calculations, leads to a systematic suppression of the metastable solutions, thus allowing a more precise estimation of the crust-core transition density and pressure, and therefore a better estimation of the crustal radius.

PHYSICAL REVIEW C 107, 045806 (2023)

arXiv:2212.09355v1 [nucl-th] 19 Dec 2022

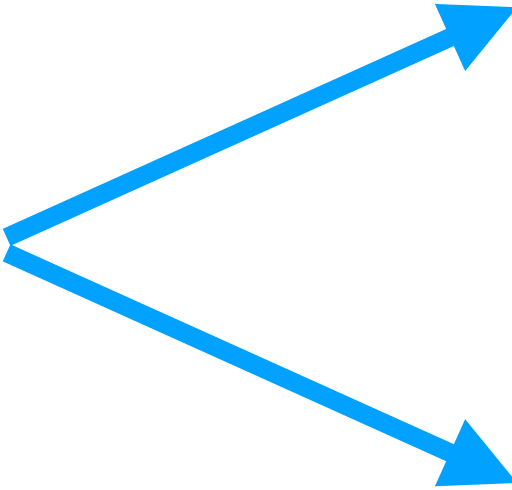
Thank you for the attention !

Relativistic Mean Field Models

$$\mathcal{L} = \sum_{i=p,n} \mathcal{L}_i + \mathcal{L}_e + \mathcal{L}_\sigma + \mathcal{L}_\omega + \mathcal{L}_\rho + \mathcal{L}_{nl} + \mathcal{L}_A$$

$$\mathcal{L}_e = \bar{\psi}_e \left[\gamma_\mu (i\partial^\mu + eA^\mu) - m_e \right] \psi_e \quad \mathcal{L}_A = -\frac{1}{4} F_{\mu\nu} F^{\mu\nu}$$

$$\mathcal{L}_i = \bar{\psi}_i \left[\gamma_\mu iD^\mu - M^* \right] \psi_i$$



$$iD^\mu = i\partial^\mu - g_\omega V^\mu - \frac{g_\rho}{2} \boldsymbol{\tau} \cdot \mathbf{b}^\mu - \frac{1 + \tau_3}{2} eA^\mu$$

$$M^* = M - g_\sigma \phi$$

Mesonic Lagrangian

$$\mathcal{L} = \sum_{i=p,n} \mathcal{L}_i + \mathcal{L}_e + \mathcal{L}_\sigma + \mathcal{L}_\omega + \mathcal{L}_\rho + \mathcal{L}_{nl} + \mathcal{L}_A$$

$$\mathcal{L}_\sigma = \frac{1}{2} \left(\partial_\mu \phi \partial^\mu \phi - m_\sigma^2 \phi^2 - \frac{1}{3} \kappa \phi^3 - \frac{1}{12} \lambda \phi^4 \right)$$

Iso-Scalar / Scalar

$$\mathcal{L}_\omega = -\frac{1}{4} \Omega_{\mu\nu} \Omega^{\mu\nu} + \frac{1}{2} m_\omega^2 V_\mu V^\mu + \frac{\xi}{4!} g_\omega^4 (V_\mu V^\mu)^2$$

Iso-Scalar / Vector

$$\mathcal{L}_\rho = -\frac{1}{4} \mathbf{B}_{\mu\nu} \cdot \mathbf{B}^{\mu\nu} + \frac{1}{2} m_\rho^2 \mathbf{b}_\mu \cdot \mathbf{b}^\mu$$

Iso-Vector / Vector

$$\mathcal{L}_{nl} = \Lambda_{\omega\rho} g_\omega^2 g_\rho^2 V_\mu V^\mu \mathbf{b}_\mu \cdot \mathbf{b}^\mu$$

Present only in the NL3 $\omega\rho$ model

RMF densities and energy density

The scalar and vector densities for the nucleons are given by :

$$\rho_{s,p} = \frac{q_p B M^*}{2\pi^2} \sum_{\nu=0}^{\nu_{\max}^p} g_s \ln \left| \frac{k_{F,\nu}^p + E_F^p}{\sqrt{M^{*2} + 2\nu q_p B}} \right|$$

$$\rho_p = \frac{q_p B}{2\pi^2} \sum_{\nu=0}^{\nu_{\max}^p} g_s k_{F,\nu}^p$$

$$\rho_{s,n} = \frac{M^*}{2\pi^2} \left[E_F^n k_F^n - M^{*2} \ln \left| \frac{k_F^n + E_F^n}{M^*} \right| \right]$$

$$\rho_n = \frac{k_F^{n3}}{3\pi^2}$$

Where $\nu_{\max}^p = \frac{E_F^{p2} - M^{*2}}{2q_p B}$, $k_{F,\nu}^p = \sqrt{E_F^{p2} - M^{*2} - 2\nu q_p B}$, $k_F^n = \sqrt{E_F^{n2} - M^{*2}}$

RMF densities and energy density

The energy density is given by :

$$\mathcal{E} = \mathcal{E}_f + \mathcal{E}_p + \mathcal{E}_n$$

Where

$$\mathcal{E}_n = \frac{1}{4\pi^2} \left[k_F^n E_F^{n3} - \frac{1}{2} M^* \left(M^* k_F^n E_F^n + M^{*3} \ln \left| \frac{k_F^n + E_F^n}{M^*} \right| \right) \right]$$

$$\mathcal{E}_p = \frac{q_p B}{4\pi^2} \sum_{\nu=0}^{\nu_{\max}} g_s \left[k_{F,\nu}^p E_F^p + \left(M^{*2} + 2\nu q_p B \right) \cdot \ln \left| \frac{k_{F,\nu}^p + E_F^p}{\sqrt{M^{*2} + 2\nu q_p B}} \right| \right]$$

$$\mathcal{E}_f = \frac{m_\omega^2}{2} V_0^2 + \frac{\xi g_v^4}{8} V_0^4 + \frac{m_\rho^2}{2} b_0^2 + \frac{m_\sigma^2}{2} \phi_0^2 + \frac{\kappa}{6} \phi_0^3 + \frac{\lambda}{24} \phi_0^4 + 3\lambda_{\omega\rho} g_\rho^2 g_\omega^2 V_0^2 b_0^2$$

Pasta Phases Calculation Details

Starting from $\mathcal{E} = f\mathcal{E}^I + (1 - f)\mathcal{E}^{II} + \mathcal{E}_{Coul} + \mathcal{E}_{surf} + \mathcal{E}_e.$

With $\mathcal{E}_{Coul} = 2\alpha e^2 \pi \Phi R_d^2 (\rho_p^I - \rho_p^{II})^2$ $\mathcal{E}_{surf} = \frac{\sigma \alpha D}{R_d}$

Minimizing with respect to the radius of clusters we get

$$\mathcal{E}_{Coul} = \frac{2\alpha}{4^{2/3}} (e^2 \pi \Phi)^{1/3} [\sigma D (\rho_p^I - \rho_p^{II})]^{2/3}$$

$$\mathcal{E}_{surf} = 2\mathcal{E}_{Coul}$$

$$R_d = \left[\frac{\sigma D}{4\pi e^2 \Phi (\rho_p^I - \rho_p^{II})^2} \right]^{1/3}$$

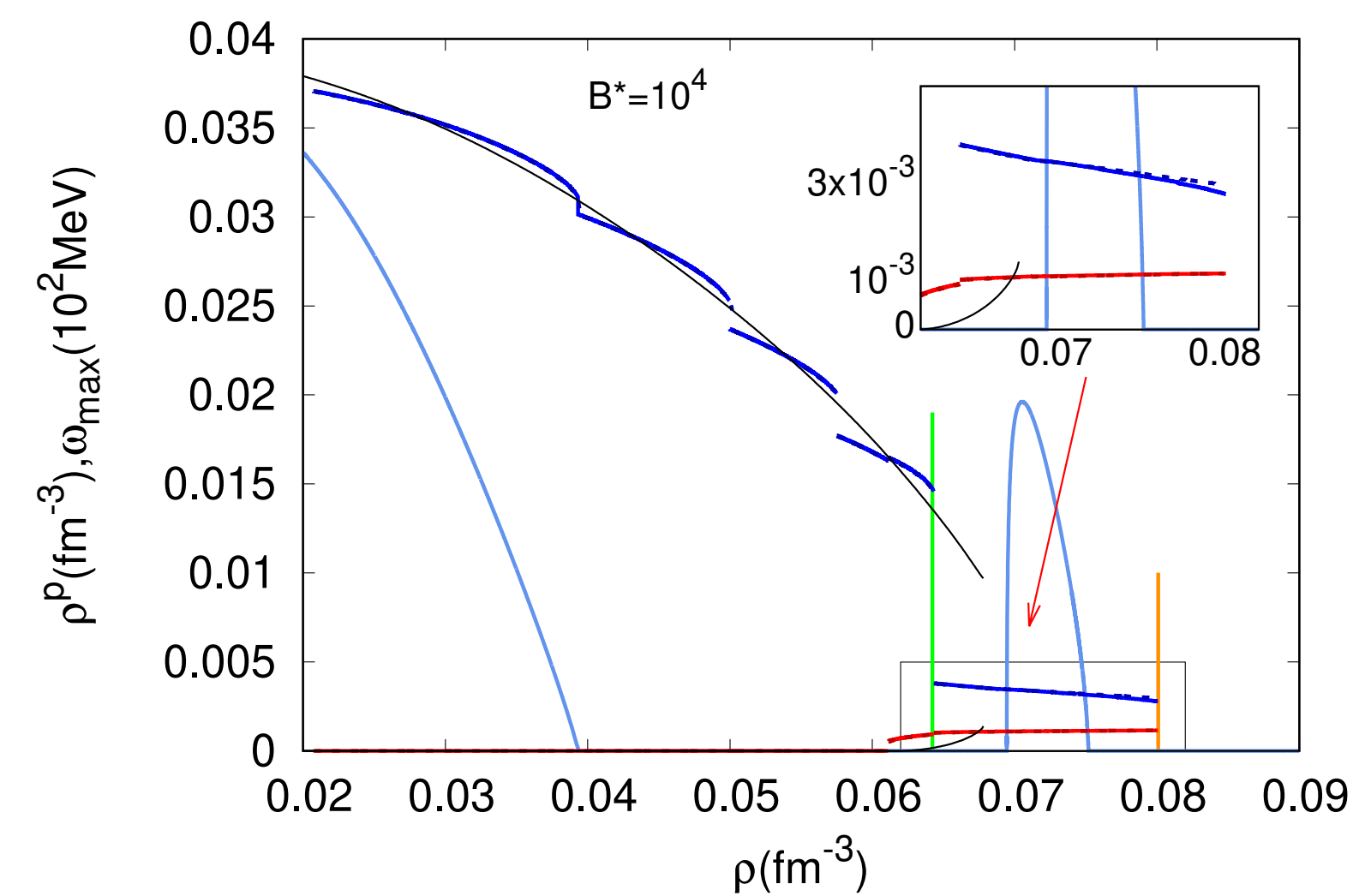
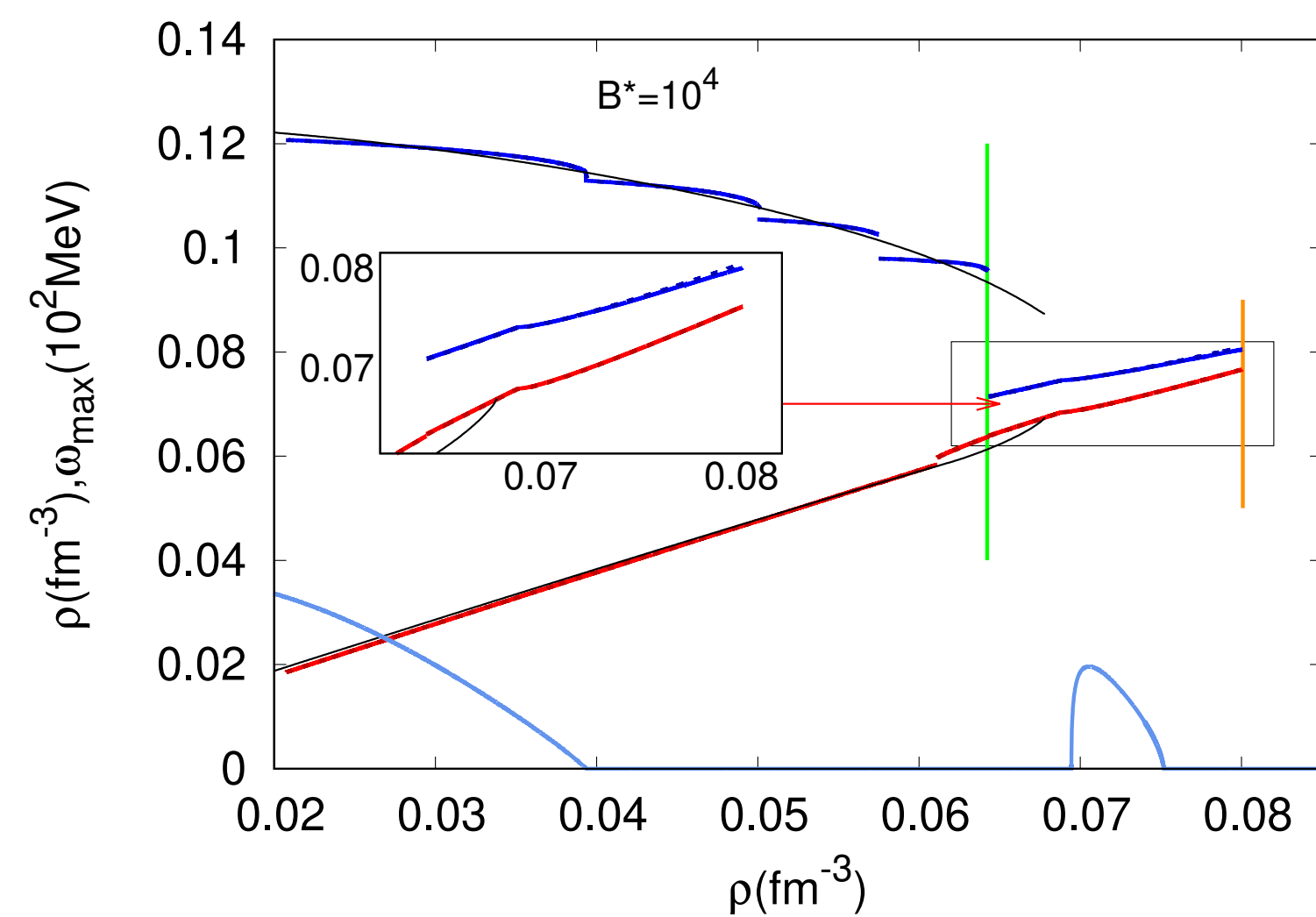
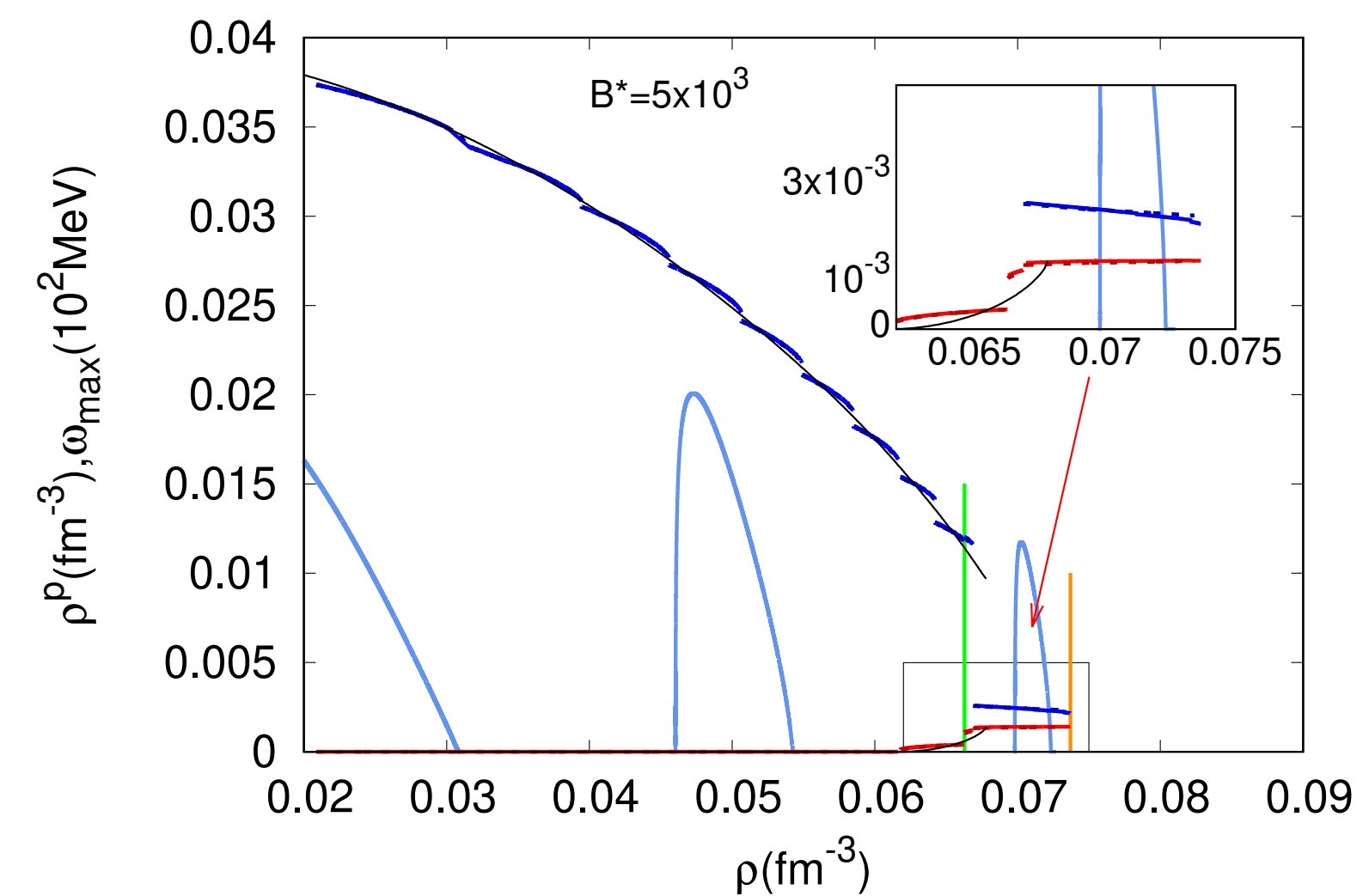
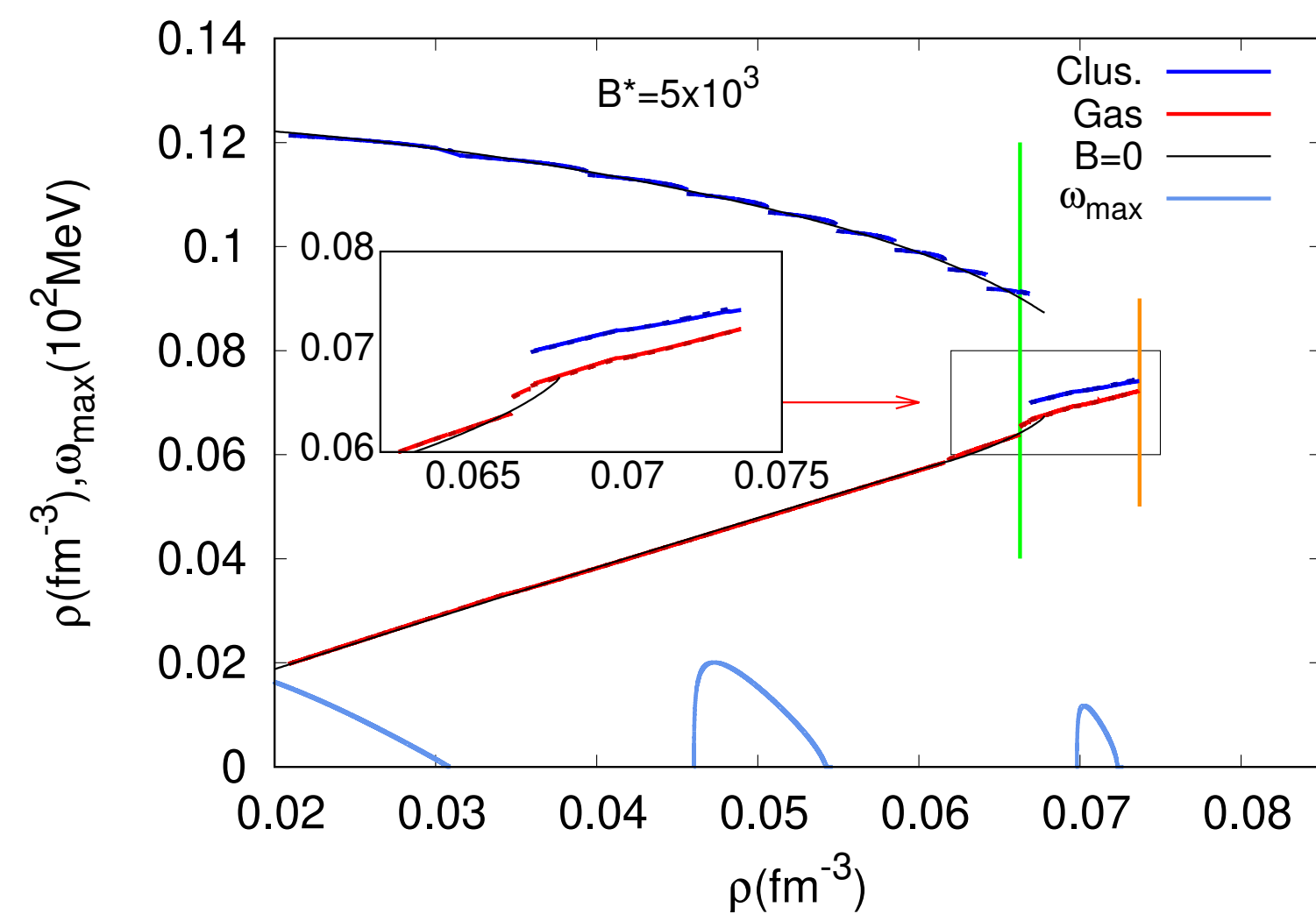
Pasta Phases Calculation Details

Other definitions:

$$\left\{ \begin{array}{l} \Phi = \left(\frac{2 - D\alpha^{1-2/D}}{D-2} + \alpha \right) \frac{1}{D+2}, \quad D = 1,3 \\ \Phi = \frac{\alpha - 1 - \ln \alpha}{D+2}, \quad D = 2 \end{array} \right.$$

$$\left\{ \begin{array}{l} \alpha = f \quad \longrightarrow \quad \text{Drops, Rods, Slabs} \\ \alpha = 1 - f \quad \longrightarrow \quad \text{Tubes, Bubbles} \end{array} \right.$$

Extended Region with Different B Values



Mass and Radius Contributions

			$M_1(M_\odot)$	$M_2(M_\odot)$	$R_T(km)$	$\Delta R_1(km)$	$\Delta R_2(km)$
$M_T = 1.4M_\odot$	NL3	$B = 0$	0.0588	0.0	14.685	1.4270	0.0
		$B^* = 5 \times 10^3$	0.0597	0.0258	14.908	1.6532	0.1541
		$B^* = 10^4$	0.0574	0.0414	15.025	1.7427	0.3148
	NL3 $\omega\rho$	$B=0$	0.0457	0.0	13.747	1.3665	0.0
		$B^* = 5 \times 10^3$	0.0526	0.0	13.871	1.5431	0.0
		$B^* = 10^4$	0.0526	0.0	13.991	1.6556	0.0
$M_T = 2.0M_\odot$	NL3	$B = 0$	0.0394	0.0	14.777	0.8691	0.0
		$B^* = 5 \times 10^3$	0.0400	0.0132	14.914	1.0064	0.0932
		$B^* = 10^4$	0.0385	0.0288	14.989	1.0617	0.1973
	NL3 $\omega\rho$	$B=0$	0.0326	0.0	14.079	0.8632	0.0
		$B^* = 5 \times 10^3$	0.0384	0.0	14.161	0.9769	0.0
		$B^* = 10^4$	0.0383	0.0	14.234	1.0437	0.0